Density functional theory study of the effects of substituents on the carbon-13 nuclear magnetic resonance chemical shifts of asphaltene model compounds

Oliveira, Jackeline S. C.; Da Costa, Leonardo M.; Stoyanov, Stanislav R.; Seidl, Peter R.

National Research Council Canada

Conseil national de recherches Canada

Canada

Density Functional Theory Study of the Effects of Substituents on the Carbon-13 Nuclear Magnetic Resonance Chemical Shifts of Asphaltene Model Compounds

Jackeline S. C. Oliveira,[†] Leonardo M. da Costa,[‡,§] Stanislav R. Stoyanov,*[,‖,⊥,#] and Peter R. Seidl*[,†]

[†]School of Chemistry, Federal University of Rio de Janeiro (UFRJ), Rio de Janeiro, Rio de Janeiro 21941-900, Brazil

[‡]Centro Universitário Estadual da Zona Oeste (UEZO), Avenida Manuel Caldeira de Alvarenga, 1203, Campo Grande, Rio de Janeiro, Rio de Janeiro 23070-200, Brazil

[§]Postgraduate Program, School of Chemistry, Federal University of Rio de Janeiro (UFRJ), Rio de Janeiro, Rio de Janeiro 21941-900, Brazil

[‖]Department of Mechanical Engineering, University of Alberta, Edmonton, Alberta T6G 2G8, Canada

[⊥]National Institute for Nanotechnology (NINT), National Research Council of Canada, Edmonton, Alberta T6G 2M9, Canada

[#]Department of Chemical and Materials Engineering, University of Alberta, Edmonton, Alberta T6G 2V4, Canada

ABSTRACT: Petroleum asphaltenes are a complex mixture of organic molecules containing mainly fused polyaromatic and naphthenic systems and pendant chains, polar moieties with heteroatoms (S, N, and O), and transition metals. A variety of spectroscopic techniques has been employed to characterize asphaltenes, but their structures remain largely elusive because of the complexity, variety of samples, and assignment limitations. Carbon-13 nuclear magnetic resonance (^{13}C NMR) spectroscopy has contributed extensively to asphaltene characterization. However, proper assignment of ^{13}C NMR spectra is very challenging because spectra of natural asphaltenes feature a large number of peaks in unusual environments, which may be hard to assign and interpret. We employ the dispersion-corrected ωB97X-D density functional with 6-31G(d,p) basis set to rationalize common trends in the ^{13}C NMR chemical shifts of asphaltene model compounds. The calculated ^{13}C NMR chemical shifts for a calibration series of 14 aromatic and heterocyclic reference compounds containing C atoms of types similar to those in the asphaltene model compounds are found to correlate linearly with the respective experimental values. The linear fitting yields a correlation coefficient of $R^2 = 0.99$ and absolute errors of less than 10 ppm. Moreover, we calculate and calibrate the ^{13}C chemical shifts of asphaltenes extracted from Brazilian vacuum residues to analyze and correlate the C atom types with those of the reference compounds. It is found that the presence of heteroatoms as well as environments with a high aromatic condensation index can significantly affect the chemical shifts. The effect of heteroatoms on the chemical shift, a situation that has scarcely been addressed in the literature, is evaluated here in detail. The results are intended to help interpret ^{13}C NMR spectra and allow for a more complete characterization of asphaltene molecules.

1. INTRODUCTION

In the last few decades, the petroleum industry has been facing a serious problem with organic deposition that occurs along almost the entire oil extraction process.[1,2] The heaviest fraction of petroleum, known to contain substances referred to as asphaltenes, is considered to be the cause of this precipitation behavior.[3] Asphaltene molecules have a strong tendency to associate and form aggregated systems that deposit in the walls of pipelines, surface facilities, reservoirs, and wellbores, thus drastically reducing petroleum recovery.[4] Asphaltenes are a complex mixture of heavy organic molecules containing fused polyaromatic and naphthenic rings, alkyl side chains, polar functional groups, transition metals (V, Ni, and Fe), and heteroatoms, such as O, N, and S.[5] In the literature, asphaltenes have been represented as island (also referred to as continental) and archipelago model structures,[6] as shown in the examples in Figure 1. To describe the complexity of asphaltene aggregation, Gray et al. have proposed a supramolecular assembly model that combines cooperative binding by hydrogen bonding, $\pi-\pi$ stacking, acid–base interactions, and metal coordination as well

as the formation of hydrophobic pockets, porous networks, and host–guest complexes.[7]

In chemistry, one of the most important goals of research studies is to determine the structure of a molecular system and to understand the relation to its chemical properties. From the experimental side, there are a larger number of useful tools available, such as nuclear magnetic resonance (NMR), microwave, infrared (IR), Raman, and single-crystal X-ray spectroscopy and neutron diffraction. Among these experimental techniques used to characterize large aromatic systems, NMR spectroscopy represents a powerful tool for describing the way atoms are bonded in molecules.[8] Recent works on characterization of different types of asphaltenes by NMR[9,10] confirm their island-type structures. These results are in a good
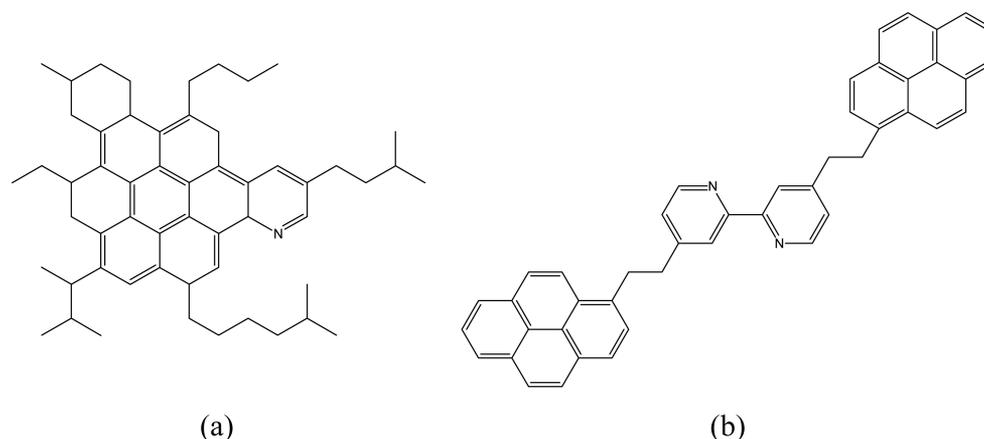
Figure 1. (a) Continental and (b) archipelago macrostructural arrangements of asphaltenes.

agreement with our original proposal[11] that representative asphaltene structures obtained from vacuum residues of petroleum from Brazilian offshore fields can be generated by NMR and elemental analyses.

In view of the enormous diversity of heavy petroleum constituents,[3] model compounds are instrumental in studies aimed at an improved understanding of the association behavior and structure of asphaltenes. Gray et al. have synthesized several model compounds containing polyaromatic π-stacking and heterocyclic hydrogen bonding sites linked by aliphatic tethers.[12] These model compounds mimic the aggregation behavior of asphaltenes in dilute and concentrated solutions and other physical properties, as characterized using ^{1}H NMR spectra and fluorescence spectroscopy. To help understand the aggregation behavior of these compounds in solution as well as to study the effect of trace amounts of water on asphaltene aggregation, we have employed a multiscale modeling approach based on density functional theory (DFT) and the 3D-RISM-KH molecular theory of solvation.[13] We have also studied the relative contributions of hydrogen-bonding and π−π stacking interactions on asphaltene aggregation in chloroform solvent[14] as well as the contributions of steric effects and dispersion interactions in a series of dimers and trimers of model hydrocarbons containing fused aromatic and cyclohexyl rings.[15] The role of transition metals in the aggregation and visible spectroscopy of asphaltenes was also investigated[16] to address the origin of the black color of bitumen (a very heavy, asphaltene-rich petroleum) and propose approaches to remove transition metals in early stages of heavy oil processing.[17]

Studies by Gillet et al.[18] and Calemma et al.[19] provide important information about the nature of the aromatic rings and the reliability of NMR analysis. It has been shown that the number of aromatic cycles per molecule is around 7, in agreement with Andrew et al.[20] and the Yen modified model[21] but diverging from the conclusions of Sheremata et al.[22] and Massuda et al.,[23] who estimate the number of fused rings at 4. However, as we have previously pointed out, recent ^{13}C NMR and two-dimensional (2D) heteronuclear single-quantum coherence (HSQC) studies[9,10] with narrow bands support the model containing 6−7 aromatic rings. It is worth noting that these discrepancies arise from the assignment of chemical shifts, and despite all of this extensive research effort, the molecular characterization of asphaltenes remains a challenging

task for the chemists, especially because of overlap of the bands attributed to different chemical structures.[24]

From a theoretical point of view, the ^{13}C NMR is an important tool in the characterization of molecular structures. Nowadays, there are a large number of calculated ^{13}C NMR spectra of high-molecular-weight organic molecules.[25,26] Brown and Ladner have employed the ^{13}C NMR technique to investigate the composition of asphaltene and heavy oil products in terms of aromatic and aliphatic compounds.[25] Using ^{13}C NMR spectra, Speight has identified various representative chemical structures of asphaltenes.[27] It has been demonstrated that, from the areas under the observed bands, it is possible to deduce average structural parameters, making ^{13}C NMR attractive for the qualitative identification of asphaltene molecular structures. Using this approach, Sato[28] has proposed chemical structures for Khafji asphaltene deduced from the analysis of the ^{1}H and ^{13}C NMR spectra.

Electronic structure calculations have found rather limited application to modeling of asphaltene nanoaggregation mainly because the methods applicable to systems as large as several nanometers, such as DFT, do not properly account for dispersion interactions. Several corrections have been proposed to remedy this deficiency of DFT, such as the inclusion of van der Waals terms in the interaction energy (DFT-D) of Grimme et al.[29] and the inclusion of C atom-centered dispersion-correcting potentials.[30] In a recent comparative study of the performance of several dispersion correction methods to DFT with respect to calculation of thermochemistry, we came to the conclusion that the results obtained using ωB97X-D by Grimme et al. are in the closest agreement and correlated well with the crystal structures of polycyclic aromatic hydrocarbons.[31] It should be noted that inclusion of dispersion terms in density functionals addresses the concern by Ruiz-Morales that the interpretation of asphaltene NMR spectra could be inadequate unless aromaticity is properly taken into account (see below).[32]

In this study, we calculated the ^{13}C NMR spectra of a calibration series of 14 compounds, including small and large aromatic hydrocarbons with and without heteroatoms as well as naphthenic compounds with high and low aromatic condensation index (CI/C1) that are typically found in asphaltene molecules. Subsequently, we calculated and calibrated the ^{13}C spectra of four continental asphaltene model compounds extracted from a sample of Brazilian vacuum residue[33] to elucidate the aromatic C atom types and correlate with the
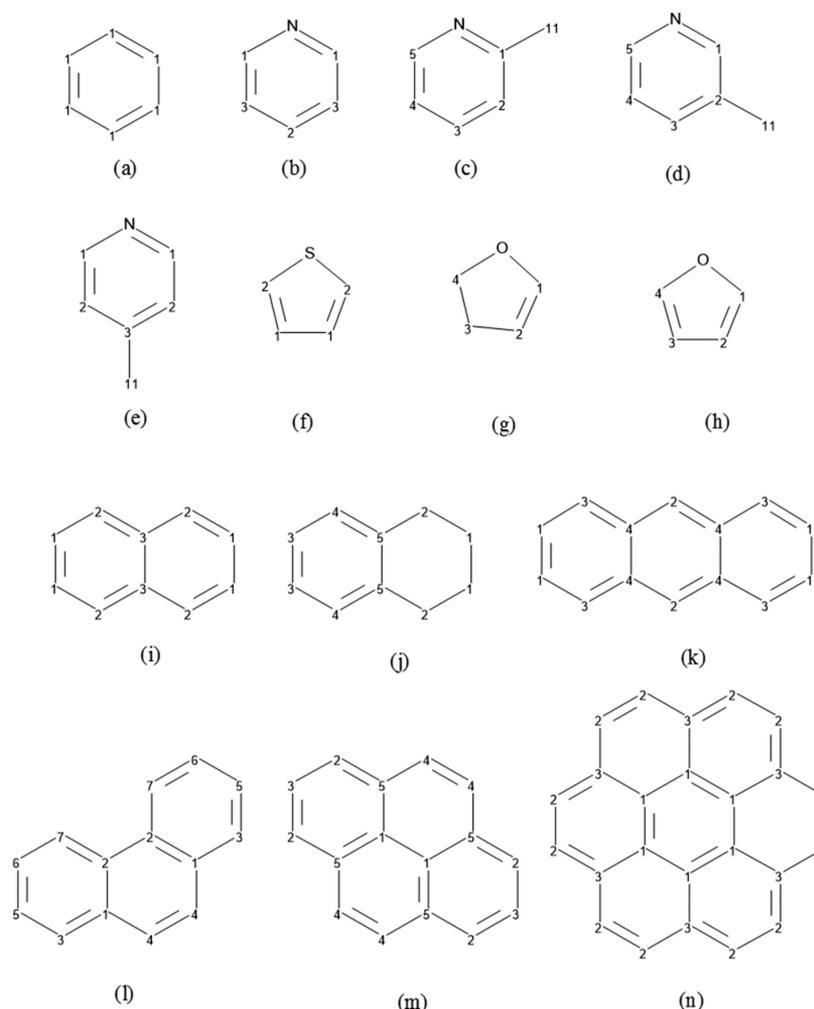
Figure 2. Asphaltene model compounds included in the calibration series: (a) benzene, (b) pyridine, (c) 2-methylpyridine, (d) 3-methylpyridine, (e) 4-methylpyridine, (f) thiophene, (g) 2,3-dihydrofuran, (h) furan, (i) naphthalene, (j) tetralin, (k) anthracene, (l) phenanthrene, (m) pyrene, and (n) coronene.

experimental chemical shift region to help the experimentalists correctly interpret ^{13}C NMR spectra.

2. COMPUTATIONAL DETAILS

The DFT calculations were performed using the ωB97X-D[34] functional and the 6-31G(d,p) basis set[35] using the Gaussian 09 computational chemistry software.[36] This combination of functional and basis set has been extensively validated and employed by us in recent works on petroleum asphaltenes.[31,37] After each geometry optimization, we calculated the normal vibration modes, to confirm that each optimized structure is a global minimum in the potential energy surface. For the ^{13}C chemical shifts, we employed the gauge-independent atomic orbital (GIAO) method.[38,39] The effect of chloroform solvent on the NMR chemical shifts is accounted for using the conductor-like polarizable continuum model (CPCM) of solvation.[40,41] Chloroform was used as a solvent because it is nonpolar and non-coordinating, has no hydrogen bonding sites, and provides a good contrast for π density.[7]

3. RESULTS AND DISCUSSION

3.1. Computational Method Calibration. The geometries of the 14 aromatic compounds, shown in Figure 2, constituting our calibration series were fully optimized in chloroform solvent using the ωB97X-D/6-31G(d,p) and PCM methods. After each optimization, the second Hessian matrix

was calculated to confirm the absence of imaginary frequencies and ensure that the optimized geometries of these compounds correspond to minima of the potential energy surface. Confident that the geometries were optimized, we performed ^{13}C NMR calculations in chloroform using the GIAO and PCM methods. As expected, there are two very distinct spectral regions, one corresponding to saturated C atoms, including aliphatic and naphthenic groups, and the other corresponding to aromatic C atoms. Each region has a distinct and relatively narrow ^{13}C chemical shift range as postulated in ref 8. It is important to note that heteroatoms shift adjacent C atoms to lower fields.

Figure 3 shows the calibration plot of the calculated and experimental ^{13}C chemical shift values for the compounds presented in Figure 2. The ^{13}C chemical shifts of saturated chain/naphthenic C atoms fall in the lower region of the graph, while aromatic C atoms are concentrated at higher values. Between the aromatic and saturated/naphthenic regions, there is a large gap that allows these C atom types to be clearly distinguished. The linear fitting correlation coefficient between the calculated and experimental ^{13}C NMR chemical shifts found is $R^2 = 0.99$, indicating an excellent correlation between this two sets of values. The slope is close to unity, and the intercept is small, indicating a very close agreement between
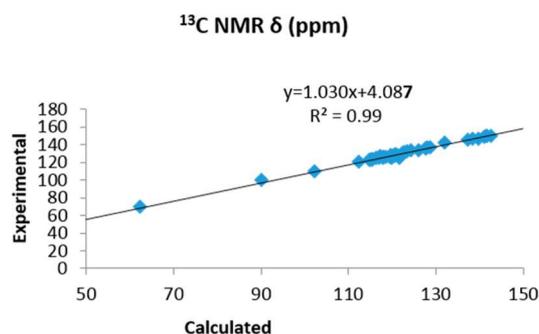
Figure 3. Linear dependence between the calculated and experimental ^{13}C NMR chemical shifts δ (ppm) for the calibration series of 14 molecules shown in Figure 2.

calculated and experimental chemical shifts (inset of Figure 3). Calibration based on this linear fitting correlation is applied to the asphaltenes studied in the next subsection.

In Table 1, we list the calculated and experimentally measured ^{13}C chemical shifts of the C atoms of the calibrations series shown in Figure 2. The chemical shifts of aliphatic and naphthenic C atoms are in the 14−70 ppm range, in agreement with the experimental band of 0−70 ppm.[9] It is important to note that the C_{naph} region (20−45 ppm) is found in the C_{aliph} region (0−70 ppm) and cannot be distinguished here. The chemical shifts of aromatic nuclei (C_{ar}) are in the 112−151 ppm range, in agreement with the observed band between 118 and 160 ppm.[9] The absolute errors, also listed in Table 1, show that the calculated chemical shifts are, in general, 7.89 ± 1.51 ppm lower than the experimental values. This result is in agreement with previous NMR studies.[42−55] The error associated with the aliphatic/naphthenic structures is 4.50 ± 2.18 ppm, whereas for the aromatic compounds, it is 8.00 ± 1.06 ppm. This shows that calculations on chemical shifts of π-electronic systems are not as precise as for the aliphatic and naphthenic compounds and demonstrates the importance of the calibration curve to obtain the theoretical chemical shift values. In both the aromatic and naphthenic groups, the presence of heteroatoms (O, N, and S) in the structure apparently does not lead to significant changes, with variations being lower than 1 ppm, in terms of absolute errors when compared to the aromatic hydrocarbon structures. This is a very important point to consider, especially in the study of asphaltenes that contain large percentages of O, N, and S heteroatoms. The average error in ^{13}C chemical shifts of small hydrocarbons (benzene, naphthalene, and phenanthrene) is 7.90 ± 1.00 ppm, whereas for the larger hydrocarbons (pyrene and coronene), it is 7.63 ± 0.69 ppm. This result shows that the errors are consistent for calculation of ^{13}C chemical shifts for small and large hydrocarbons.

Benzene rings are found in major sources of raw material for a large number of chemical processes, making the correct characterization of benzene derivatives extremely important. One of the most precise characterization techniques for benzene derivatives is ^{13}C NMR. A wide array of substituents, such as alkyl groups, aromatic rings, and heteroatoms, can change the chemical shift of C nuclei on the benzene ring (C_a), as documented in the literature. Alkyl substitution in the benzene ring increases the steric repulsion and is directly correlated with the alkyl group size. The presence of the methyl group in toluene increases the chemical shift of the substituted C nucleus by 9.2 ppm relative to benzene. Increasing the size of

Table 1. Calculated and Experimental ^{13}C Chemical Shifts δ (ppm) for the 14 Asphaltene Model Compounds Shown in Figure 2 and Absolute Errors (|Calc. − Exp.|)

compound	atom	type	δ (calc.)	δ (exp.)	|calc. − exp.|
benzene[42]	1	C_{ah}	119.70	128.36	8.66
pyridine[43]	1	C_{ah}	149.94	141.78	8.16
	2	C_{ah}	135.89	127.65	8.24
	3	C_{ah}	123.75	115.49	8.26
2-methylpyridine[44]	1	C_{al}	158.29	151.36	6.93
	2	C_{ah}	123.27	115.10	8.17
	3	C_{ah}	136.28	127.78	8.50
	4	C_{ah}	120.72	112.49	8.23
	5	C_{ah}	149.00	141.13	7.87
	6	C_{met}	24.30	19.73	4.57
3-methylpyridine[45]	1	C_{ah}	142.64	150.27	7.63
	2	C_{al}	126.15	133.08	6.93
	3	C_{ah}	128.09	136.40	8.31
	4	C_{ah}	115.12	123.16	8.04
	5	C_{ah}	138.50	146.93	8.43
	6	C_{met}	14.44	18.36	3.92
4-methylpyridine[46]	1	C_{ah}	141.52	149.60	8.08
	2	C_{ah}	116.45	124.63	8.18
	3	C_{al}	139.66	146.93	7.27
	4	C_{met}	16.39	20.89	4.50
thiophene[47]	1	C_{ah}	117.33	126.82	9.49
	2	C_{ah}	121.74	125.08	3.34
2,3-dihydrofuran[48]	1	C_{ins}	137.42	145.99	8.57
	2	C_{ins}	90.05	99.54	9.49
	3	C_{naph}	62.22	69.58	7.36
	4	C_{naph}	25.18	29.28	4.10
furan[49]	1	C_{ah}	102.25	109.54	7.29
	2	C_{ah}	132.05	142.64	10.59
naphthalene[50]	1	C_{ah}	117.95	125.75	7.80
	2	C_{ah}	120.36	127.84	7.48
	3	C_{aj2}	124.19	133.45	9.26
tetralin[51]	1	C_{naph}	18.80	23.26	4.46
	2	C_{naph}	25.34	29.39	4.05
	3	C_{ah}	117.06	125.43	8.37
	4	C_{ah}	120.73	129.11	8.38
	5	C_{al}	128.73	137.07	8.34
anthracene[52]	1	C_{ah}	119.84	125.33	5.49
	2	C_{ah}	117.82	126.21	8.39
	3	C_{ah}	120.92	128.16	7.24
	4	C_{aj2}	122.80	131.70	8.90
phenanthrene[53]	1	C_{aj2}	123.38	131.99	8.61
	2	C_{aj2}	122.21	130.25	8.04
	3	C_{ah}	121.28	128.46	7.18
	4	C_{ah}	120.14	126.84	6.70
	5	C_{ah}	118.46	126.46	8.00
	6	C_{ah}	118.69	NA[a]	–
	7	C_{ah}	115.44	122.59	7.15
pyrene[54]	1	C_{aj3}	116.35	124.58	8.23
	2	C_{ah}	117.97	124.81	6.84
	3	C_{ah}	118.13	125.70	7.57
	4	C_{ah}	120.59	127.25	6.66
	5	C_{aj2}	122.68	131.04	8.36
coronene[55]	1	C_{aj3}	114.90	122.53	7.63
	2	C_{ah}	119.52	126.10	6.58
	3	C_{aj2}	120.83	128.72	7.89

[a]NA = not available.
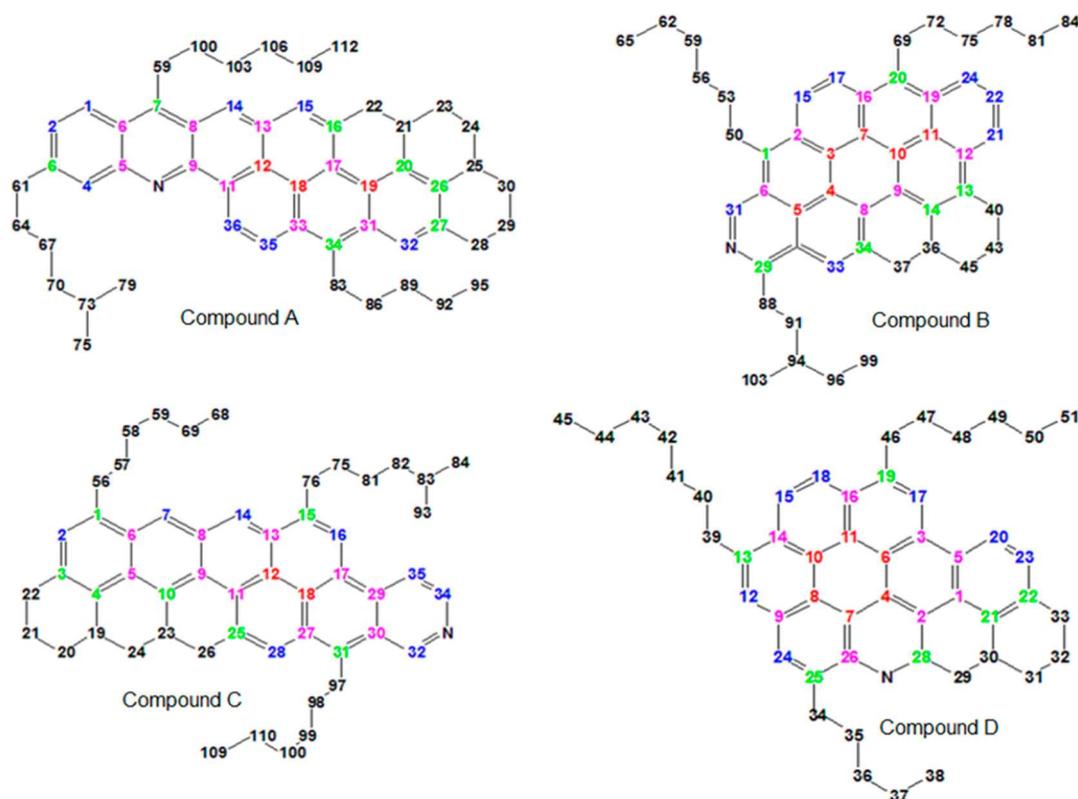
Figure 4. Continental asphaltene model compounds A−D with aliphatic (C_{aliph}) and naphthenic (C_{naph}) C atoms in black, aromatic C bonded to a H atom (C_{ah}) in blue, aromatic C atoms at junctions of two rings (C_{aj2}) in pink, aromatic C atoms at junctions of three rings (C_{aj3}) in red, and C atoms at junctions of aromatic and naphthenic rings (C_{an}) and alkyl-substituted aromatic C atoms (C_{al}) in green.

the substituent to ethyl, isopropyl, and t-butyl groups changes the chemical shifts by 15.6, 20.3, and 22.3 ppm relative to benzene. The chemical bond length between the substituted C and the branch is strictly correlated with the change in the ^{13}C chemical shift. The larger steric repulsion promotes elongation of the chemical bond, thus decreasing the electron density at the C nucleus and deshielding it, and the chemical shift increases to a lower field. The bond lengths observed in ethylbenzene, isopropylbenzene, and $tert$-butylbenzene are 1.51, 1.52, and 1.53 Å, respectively. The size of the aromatic ring is also correlated with the change of the chemical shift of the nuclei. In this case, the charge on the nuclei is extremely important to justify the shielding or deshielding behavior. The ^{13}C chemical shift of benzene is 128.36 ppm. In naphthalene, we note two ^{13}C NMR trends. First, the C_1 and C_2 atoms have a negative charge, showing that these are shielded and providing a rationalization for the lower chemical shifts than benzene. Second, the C_3 nuclei have a higher chemical shift than the benzene ring. These atoms have positive partial charges, thus, are deshielded, and correspond to a lower chemical shift. The same behavior is found in anthracene and phenanthrene, where the peripheral C atoms have negative charges and nuclei are more shielded than those in benzene and have lower chemical shifts relative to benzene. The core C atoms have positive charges, and their nuclei are more shielded and have lower chemical shifts. In pyrene, the behavior reported above is also found, except that the C_1 atom has a negative charge, with its nucleus being shielded, and has a lower chemical shift than the C_5 atom. The C_1 atom differs from the junction C atoms discussed above because of its higher aromatic condensation index and a more negative charge.

Comparison between the chemical shifts of the benzene and pyridine rings highlights three characteristic features. First, the C_1 nuclei of pyridine has larger chemical shifts than those in benzene, because of the inductive effect of the N atom that withdraws electron density and deshields the C_1 nuclei. Second, the C_3 nucleus of pyridine has a lower chemical shift than benzene C nuclei. This is due to the positions of the positive charges in the resonance structures.

A comparison of pyridine, 2-methylpyridine, 3-methylpyridine, and 4-methylpyridine shows interesting trends. The C_1 nucleus has the largest chemical shift (150 ppm), independent of the position of the substituent. A discussion of specific effects is beyond the scope of the present paper, but it is worth noting that all C atoms are deshielded and show larger chemical shifts and that the C atom directly bonded to the substituent undergoes the largest chemical shift increase (around 16 ppm) compared to the non-substituted C atoms.

Analysis of furan and thiophene heterocyclic aromatic compounds shows that the C atoms adjacent to the O atom of furan have a larger chemical shift (143 ppm) than the corresponding atoms in thiophene (125 ppm). The O atom is more electronegative than the S atom and deshields the neighboring atoms more than the S atom. The aromatic O−C chemical bond in the furan ring is 1.36 Å, which is shorter than the corresponding bond in thiophene (1.71 Å). The shorter aromatic O−C bond in furan arises from the increased electron density on the C atoms, shielding these nuclei and increasing the chemical shift. The majority of the ^{13}C chemical shifts of polycyclic aromatic compounds are lower than those of benzene, with the exception of the C atoms bonded to H

Table 2. Calculated and Linearly Corrected (Calc.) ^{13}C NMR Chemical Shifts δ (ppm) for the Asphaltene Model Compounds A–D[a]

type	experimental	compound A atoms[a]	δ (calc.)	compound B atoms[a]	δ (calc.)	compound C atoms[a]	δ (calc.)	compound D atoms[a]	δ (calc.)
C$_{al}$	NA[b]	7	150	29	157	15	139	25	143
C$_{al}$	137–160,[9] 136.4[10]	3	148	20	137	31	137	19	143
C$_{al}$	137–160,[9] 136.4[10]	34	137	1	136	1	136	13	139
C$_{an}$	132–137,[9] 136.4[10]	16	144	34	138	25	137	28	158
C$_{an}$	132–137,[9] 136.4[10]	27	138	14	135	10	136	22	136
C$_{an}$	132–137,[9] 136.4[10]	20	136	13	132	4	133	21	135
C$_{an}$	132–137,[9] 136.4[10]	26	135	–	–	3	131	–	–
C$_{aj2}$	NA[b]	5	150	12	132	13	131	26	144
C$_{aj2}$	NA[b]	9	146	19	130	29	130	3	130
C$_{aj2}$	128–136,[9] 136.4[10]	13	134	2	128	6	129	9	128
C$_{aj2}$	128–136,[9] 136.4[10]	33	130	16	128	11	128	14	127
C$_{aj2}$	128–136,[9] 136.4[10]	11	130	8	125	8, 27	128	1	127
C$_{aj2}$	128–136,[9] 136.4[10]	31	129	9	124	5	127	16	127
C$_{aj2}$	NA[b]	6	124	6	124	17	125	5	127
C$_{aj2}$		8	123	28	123	30	125	2	118
C$_{aj2}$	NA[b]	–	–	–	–	9	123	–	–
C$_{aj3}$	123–126,[9] 122, 129[10]	12	128	5	127	18	125	4	127
C$_{aj3}$	123–126,[9] 122, 129[10]	17, 19	125	3	123	12	123	11	125
C$_{aj3}$	123–126,[9] 122, 129[10]	18	123	7	123	–	–	10	124
C$_{aj3}$	123–126,[9] 122, 129[10]	–	–	11	123	–	–	8	120
C$_{aj3}$	123–126,[9] 122, 129[10]	–	–	10	121	–	–	6	120
C$_{aj3}$	123–126,[9] 122, 129[10]	–	–	4	120	–	–	7	117
C$_{ah}$	118–130,[9] 127.0[10]	4	130	31	143	32	152	23	129
C$_{ah}$	118–130,[9] 127.0[10]	2	128	17	127	34	142	24	128
C$_{ah}$	118–130,[9] 127.0[10]	35	127	15	126	2	131	12	127
C$_{ah}$	118–130,[9] 127.0[10]	1	126	22	126	14	123	15	124
C$_{ah}$	118–130,[9] 127.0[10]	36	125	24	122	7	123	18	123
C$_{ah}$	118–130,[9] 127.0[10]	15	125	21	121	28	122	17	122
C$_{ah}$	118–130,[9] 127.0[10]	32	123	33	121	16	119	20	122
C$_{ah}$	118–130,[9] 127.0[10]	14	122	–	–	35	116	–	–
C$_{naph}$	20–45,[9] 37.3[10]	25	40	37	39	26	39	29	41
C$_{naph}$	20–45,[9] 37.3[10]	22	40	36	38	24	38	30	37
C$_{naph}$	20–45,[9] 37.3[10]	21	38	45	31	23	38	31	31
C$_{naph}$	20–45,[9] 37.3[10]	28	34	40	28	19	38	33	31
C$_{naph}$	20–45,[9] 29.9[10]	23	32	43	23	22	31	32	23
C$_{naph}$	20–45,[9] 29.9[10]	30	32	–	–	20	31	–	–
C$_{naph}$	20–45,[9] 29.9[10]	24	31	–	–	76	31	–	–
C$_{naph}$	20–45,[9] 29.9[10]	29	24	–	–	21	23	–	–
C$_{aliph}$	0–70[9]	70	39	91	38	82	38	39	37
C$_{aliph}$	0–70[9]	61	38	88	37	56	35	40	35
C$_{aliph}$	0–70[9]	64	37	53	33	98	33	46	34
C$_{aliph}$	0–70[9]	86	31	94	33	100	32	43	33
C$_{aliph}$	0–70[9]	73	30	72	32	59	31	35	33
C$_{aliph}$	0–70[9]	67	30	78	32	83	30	41	32
C$_{aliph}$	0–70[9]	100	29	96	30	99	30	42	32
C$_{aliph}$	0–70[9]	103	29	75	30	81	28	34	30
C$_{aliph}$	0–70[9]	106	28	59	30	58	28	47	30
C$_{aliph}$	0–70[9]	59	28	69	29	57	28	48	28
C$_{aliph}$	0–70[9]	89	27	56	28	97	28	36	28
C$_{aliph}$	0–70[9]	83	27	50	28	75	27	49	28
C$_{aliph}$	0–70[9]	75	25	81	24	110	25	44	25
C$_{aliph}$	0–70[9]	92	24	62	24	93	24	37	23
C$_{aliph}$	0–70[9]	109	22	103	17	69	22	50	21
C$_{aliph}$	0–70[9]	79	21	84	15	84	21	51	15
C$_{aliph}$	0–70[9]	112	21	65	13	109	15	45	15
C$_{aliph}$	0–70[9]	95	15	99	7	68	15	38	13

[a]The atom type notation is the same as in Figure 4 and the main text. [b]NA = not available.

atoms. The C atoms of compounds with high aromatic indices have lower chemical shifts.

3.2. Computational Study of Four Asphaltenes from Brazilian Vacuum Residues.

The determination of individual molecular structures of asphaltenes is a very challenging task for chemists. Many molecular features and properties of asphaltenes are well-known, and model compounds that are representative of certain structural motifs have been investigated. The arrangements of aromatic and naphthenic rings and the position of side chains and polar groups are of particular interest and can be identified by NMR in model compounds. The chemical shifts of these arrangements are calculated to probe the magnetic properties of nuclei of model compounds and better characterize the molecular structures of asphaltenes obtained from samples of interest.

The geometries of four typical asphaltene structures generated on the basis of NMR and elemental analyses of fractions of asphaltenes from vacuum residues are given in Figure 4.[33] These structures are fully optimized using the ωB97X-D/6-31G(d,p)/PCM method in the chloroform solvent and confirmed to be true potential energy surface minima. For the optimized geometries, we calculated the respective ^{13}C NMR chemical shifts in chloroform using the GIAO/PCM method. In the optimized structures of these model compounds, we distinguished seven types of distinct C nuclei, aliphatic (C_{aliph}), naphthenic (C_{naph}), aromatic bonded to a H atom (C_{ah}), aromatic at a junction of two rings (C_{aj2}), aromatic at a junction of three rings (C_{aj3}), junction of aromatic and naphthenic rings (C_{an}), and alkyl-substituted aromatic (C_{al}), that can be attributed to certain regions by NMR experiments.[9] In the four model compounds, we analyze the chemical shifts of ^{13}C nuclei influenced by the presence of heteroatoms, alicyclic side chains, naphthenic rings, and high aromatic condensation regions.

In Table 2, we list the calibrated ^{13}C chemical shifts of these four asphaltene structures. In the literature, ^{13}C chemical shift tables commonly attribute the C_{aliph} region to 0−70 ppm, the C_{naph} region to 20−45 ppm, the C_{ah} region to 118−130 ppm, the C_{aj2} region to 128−136 ppm, the C_{aj3} region to 123−126 ppm, the C_{an} region to 132−137 ppm, and the C_{al} region to 137−160 ppm.[9]

3.2.1. Analysis of the Aliphatic (C_{aliph}) and Naphthenic (C_{naph}) C Atoms.

The saturated aliphatic (C_{aliph}) and naphthenic (C_{naph}) C atoms in the four asphaltene model compounds are found in the saturated C nuclei (C_{sat}) region of 0−70 ppm. The chemical shifts of these two types of C nuclei show considerable overlap,[56] and unless additional experiments, such as those described in ref 10, are performed to determine their respective connectivities, assignments based on chemical shift regions can lead to errors in elucidating the chemical structure of a molecule.

3.2.2. Analysis of the Aromatic C Atoms Bonded to H Atoms (C_{ah}).

In model compounds A and D, the chemical shifts of the C_{ah} are in the 122−129 ppm region, in agreement with the observed experimental range. In model compound B, the chemical shifts of all C_{ah} nuclei are in the expected region, except C_{31}, which has a higher chemical shift of 143 ppm. This C atom is the only C_{ah} adjacent to a heteroatom; therefore, it is deshielded and has a larger chemical shift.[9] In model compound C, most of the ^{13}C chemical shifts are in the expected region. These results indicate that, in asphaltene compounds, if all C_{ah} chemical shifts are in the expected region, these C atoms are not adjacent to heteroatoms, as in model compounds A and D.

3.2.3. Analysis of the C Atoms at Junctions of Two Aromatic Rings (C_{aj2}).

The aromatic ring currents are mainly responsible for the large effects on chemical shifts observed in these molecules. Induced ring currents are observed in the delocalized π electrons of the aromatic ring that influence the chemical shift.[57] This effect is stronger in aromatic molecules with a high number of junction aromatic C atoms related to the total number of external aromatic or peripheral C atoms and is better known as the highest condensation index (CI/Ct).[58] In model compound A, the chemical shifts of C_{13}, C_{33}, C_{11}, and C_{31} are in the expected region of 130−134 ppm. C_5 and C_9 have higher chemical shifts of 150 and 148 ppm, respectively. The N nucleus is more electronegative than C_5 and C_9, leading to deshielding and larger chemical shifts. C_6 and C_8 have lower chemical shifts of 125 and 124 ppm, respectively, suggesting that these are subject to inductive effects of the aliphatic side chain that shields the nuclei and causes the chemical shifts to fall below the normal range.

In model compound B, the chemical shifts of the C_2, C_{12}, and C_{19} atoms are found in the 128−132 ppm region, in agreement with the expected values. C_6, C_{28}, C_8, and C_9 form longer chemical bonds than the average bonds between aromatic $C_{sp^2-sp^2}$ atoms.[9] Hence, the electron density over C_6, C_{28}, C_8, and C_9 is lower; the nuclei are deshielded; and the chemical shift is larger.

In model compound C, the chemical shifts of C_6, C_{11}, C_{13}, and C_{29} are within the expected 128−130 ppm region, whereas the chemical shifts of C_5, C_8, C_9, C_{17}, C_{27}, and C_{30} are lower (123−128 ppm) than that.[9] This behavior is likely due to the presence of the aliphatic side chain that donates electron density, shields the nuclei, and causes the chemical shifts to fall below the expected region.

In model compound D, the chemical shifts of C_1, C_3, C_5, C_9, C_{14}, and C_{16} are between 127 and 130 ppm, as expected. The C_{26} nucleus has a chemical shift of 144 ppm, because it is adjacent to the N atom that deshields it. The chemical shift of C_2 is 118 ppm, which is below the expected region. This behavior is probably due to its being part of the highly polycondensed moiety.

3.2.4. Analysis of the C Atoms at the Junction of Three Aromatic Rings (C_{aj3}).

In model compound A, the chemical shift of C_{18} is 123 ppm, which is within the experimental range of 123−126 ppm. The C_{12} atom has a chemical shift of 128 ppm, which is above the normal range. This behavior could be due to the fact that C_{12} forms longer chemical bonds than the average aromatic bond length.[9] Hence, the electron density at atom C_{12} will be decreased; the nucleus will be deshielded; and the chemical shift will be higher than normal.

Among the six C_{aj3} atoms in model compound B, four atoms (C_3, C_5, C_7, and C_{11}) have chemical shifts within the expected range (123−126 ppm) and two atoms (C_{10} = 121 ppm, and C_4 = 120 ppm) have lower chemical shifts. This deviation is probably is due to the high polyaromatic condensation index. In model compound C, the chemical shifts of both C_{18} = 125 ppm and C_{12} = 124 ppm nuclei are within the expected range of 123−126 ppm. Model compound D contains six C_{aj3} atoms. The chemical shift of two of these (C_{11} = 125 ppm, and C_{10} = 124 ppm) are within the expected range. Three C nuclei have chemical shifts that are lower than expected (C_7 = 117 ppm, and C_6 and C_8 = 120 ppm), probably because of their high aromatic condensation index, as observed in coronene (115−121 ppm).

3.2.5. Analysis of C Atoms at the Junction of Aromatic and Naphthenic Rings (C_{an}). The interpretation of chemical shifts of these types of C nuclei are very important in view of the important role of naphthenic rings upon association of model compounds of asphaltenes that we recently reported.[15] An increase in the number of aromatic rings should lead to stronger aggregation, whereas the presence and arrangement of naphthenic rings tend to weaken the $\pi-\pi$ stacking interactions between asphaltene molecules. In model compound A, the C_{an} nuclei are C_{27}, C_{26}, C_{20}, and C_{16}. In model compound B, the C_{an} atoms are C_{13}, C_{14}, and C_{34}. In model compound C, these are C_3, C_4, C_{10}, and C_{25}. In model compound D, the C_{an} atoms are C_{21}, C_{22}, and C_{28}.

In Table 2, we show that, in model compound A, C_{20} (136 ppm) and C_{26} (135 ppm) fall in the expected region, whereas C_{16} (144 ppm) and C_{27} (138 ppm) have higher chemical shifts. It is interesting to point that the C_{an} nuclei in the ring core are found in the expected chemical shift region, whereas the C_{an} nuclei in the periphery have higher chemical shifts. In model compound B, the chemical shifts of 132 and 135 ppm for C_{13} and C_{14} are in the expected region. The chemical shift of C_{34} (138 ppm) is higher than expected. C_{13} and C_{34} are peripheral nuclei, whereas C_{14} is in a position located closer to the core. In model compound C, the chemical shifts of all of the C_{an} nuclei fall in the expected region, i.e., C_3 (132 ppm), C_4 (133 ppm), C_{10} (136 ppm), and C_{25} (137 ppm). C_4 and C_{10} are in the core, whereas C_3 and C_{25} are in peripheral positions. In model compound D, the chemical shifts of C_{21} (135 ppm) and C_{22} (136 ppm) a fall in the expected region. The chemical shift of C_{28} (158 ppm) is higher than normal, because of its position adjacent to the N atom. It is clear that the positions of heteroatoms are responsible for the chemical shifts of the C_{an} nuclei that fall outside of the 132−137 ppm region. We found that the chemical shifts of some C_{an} nuclei fall very far from this region, because of either the proximity of a heteroatom or their high aromatic condensation index. It can be inferred that, when these factors are present in asphaltene molecules, the chemical shifts of C nuclei may not fall inside the normal regions.

3.2.6. Analysis of the Alkyl-Substituted Aromatic C Atoms (C_{al}). According to the literature, the chemical shifts of alkyl C nuclei are in the 137−160 ppm region. It is interesting to note that this is the only region that includes higher chemical shifts because of the presence of heteroatoms. In Table 2, we show for model compound A that C_3 (148 ppm), C_7 (150 ppm), and C_{34} (137 ppm) are in the expected region. In model compound B, C_{20} (137 ppm) and C_{29} (157 ppm) are found in the expected region, whereas C_1 (136 ppm) falls in a lower region, probably because of the presence of aliphatic side chains. This behavior was also found for C_1 (136 ppm) of model compound C. The chemical shifts of the rest of the C_{al} nuclei of model compound C fall in the expected region. In model compound D, the chemical shifts of C_{13} (139 ppm), C_{19} (143 ppm), and C_{25} (143 ppm) fall in the expected region.

4. CONCLUSION

Characterization of the molecular structures of petroleum asphaltenes remains a challenging task because of the number and complexity of the structures involved. To obtain detailed information about the structure of asphaltenes, we calculated the ^{13}C NMR chemical shifts to identify trends and help predict the structures. First, we calculate the ^{13}C NMR spectra of 14 aromatic and heterocyclic compounds and correlated the calculated chemical shifts with the experimental chemical shifts.

Linear fitting of these calculated and experimental chemical shifts yields δ (exp.) = 1.03δ (calc.) + 4.08, with a correlation coefficient R^2 of 0.99. Second, we calculated and calibrated the ^{13}C NMR of four asphaltene model compounds using the linear fitting equation.

We identified seven types of C nuclei in these asphaltene model compounds: C_{aliph}, C_{naph}, C_{ah}, C_{aj2}, C_{aj3}, C_{an}, and C_{al}. We found that C_{aliph} and C_{naph} of all four asphaltene model compounds fall in the expected region. The C_{aliph} region includes the C_{naph} region, and assignments are very difficult, requiring additional experiments as those in ref 10. C_{ah} of the four structures also fall in the expected region with the exception of C_{31} (model compound B) and C_{32} and C_{34} (model compound C) that are adjacent to heteroatoms. The C_{al} nuclei fall in the expected region, except those with a high aromatic condensation index that fall below this region. The C_{aj2}, C_{aj3}, and C_{an} nuclei fall in regions that are either higher than expected because of the presence of heteroatoms or lower than expected because of the presence of aliphatic side chains or high aromatic condensation index. All of the chemical shifts of the C_{al} nuclei fall in the expected region. This C_{al} region is very large and reflects the effects of heteroatoms and substituents as well as high condensation index on chemical shifts.

This work presents very good correlations between computational and experimental results and shows how computational insights can help avoid errors in structure prediction to comprehensively characterize asphaltene molecules. The challenges outlined in this paper highlight the necessity for further studies aimed at assignment of all C atom types and chemical effects. Thorough analysis of the effects of aromatic condensation index, heteroatoms, and substituents is very important for reliable and consistent predictions of asphaltene molecular structure based on ^{13}C NMR spectra. Advanced NMR techniques, such as solid-state ^{13}C NMR, have recently been assessed for sensitivity with respect to both two- and three-dimensional structural characterizations of petroleum asphaltenes.[59] Anisotropic tensors from computational studies could help unambiguously interpret the fingerprints of aromatic ring current effects and C atoms in proximity to heteroatoms once more experimental solid-state NMR spectra for validation and calibration become available. Improved structure characterization of heavy petroleum is important for understanding the mechanism of aggregation and surface adsorption of asphaltenes and could help propose novel approaches for controlling of organic deposition in the petroleum industry.

■ AUTHOR INFORMATION

Corresponding Authors
*E-mail: stoyanov@ualberta.ca.
*E-mail: pseidl@eq.ufrj.br.
Notes
The authors declare no competing financial interest.

■ ACKNOWLEDGMENTS

on the presentation of the results. The computations were partially performed at the Compute/Calcul Canada's Western Canada Research Grid (WestGrid) as part of the allocation of Dr. Andriy Kovalenko, Senior Research Officer at the National Institute for Nanotechnology and Adjunct Professor at the Department of Mechanical Engineering, University of Alberta, Edmonton, Alberta, Canada.

■ REFERENCES

(1) Strausz, O. P.; Lown, E. M. *The Chemistry of Alberta Oil Sands Bitumens and Heavy Oils*; Alberta Energy Research Institute (AERI): Calgary, Alberta, Canada, 2003.

(2) Sheu, E. Y. Petroleum asphaltene: Properties, characterization, and issues. *Energy Fuels* 2002, 16, 74−82.

(3) Wiehe, I. A. *Process Chemistry of Petroleum Macromolecules*; CRC Press: Boca Raton, FL, 2008.

(4) Groenzin, H.; Mullins, O. C. Molecular size and structure of asphaltenes from various sources. *Energy Fuels* 2000, 14, 677−684.

(5) Qian, K.; Mennito, A. S.; Edwards, K. E.; Ferrughelli, D. T. Observation of vanadyl porphyrins and sulfur-containing vanadyl porphyrins in a petroleum asphaltene by atmospheric pressure photoionization Fourier transform ion cyclotron resonance mass spectrometry. *Rapid Commun. Mass Spectrom.* 2008, 22, 2153−2160.

(6) Shi, Q.; Hou, D. J.; Chung, K. H.; Xu, C. M.; Zhao, S. Q.; Zhang, Y. H. Characterization of heteroatom compounds in a crude oil and saturates aromatics, resins, and asphaltenes (SARA) and non-basic nitrogen fractions analyzed by negative-ion electrospray ionization Fourier transform ion cyclotron resonance mass spectrometry. *Energy Fuels* 2010, 24, 2545−2553.

(7) Gray, M. R.; Tykwinski, R. R.; Stryker, J. M.; Tan, X. Supramolecular assembly model for aggregation of petroleum asphaltenes. *Energy Fuels* 2011, 25, 3125−3134.

(8) Silverstein, R. M.; Webster, F. X.; Kiemle, D. J. *Spectrometry Identification of Organic Compounds*; John Wiley & Sons, Inc.: Hoboken, NJ, 2005.

(9) Fergoung, T.; Bouhadda, Y. Determination of Hassi Messaoud asphaltene aromatic structure from ¹H & ¹³C NMR analysis. *Fuel* 2014, 115, 521−526.

(10) Majumdar, R. D.; Gerken, M.; Mikula, R.; Hazendonk, P. Validation of the Yen−Mullins model of Athabasca oil-sands asphaltenes using solition-state ¹H NMR relaxation and 2D HSQC spectroscopy. *Energy Fuels* 2013, 27, 6528−6537.

(11) Carauta, A. N. M.; Seidl, P. R.; Chrisman, E. C. A. N.; Correia, J. C. G.; Menechini, P. O.; Silva, D. M.; Leal, K. Z.; de Menezes, S. M. C.; de Souza, W. F.; Teixeira, M. A. G. Modeling solvent effects on asphaltene dimers. *Energy Fuels* 2005, 19, 1245−1251.

(12) Tan, X.; Fenniri, H.; Gray, M. R. Water enhances the aggregation of model asphaltenes in solution via hydrogen bonding. *Energy Fuels* 2009, 23, 3687−3693.

(13) Kovalenko, A. Three-dimensional RISM Theory for Molecular Liquids and Solid-liquid Interfaces. In *Molecular Theory of Solvation*; Hirata, F., Ed.; Series: Understanding Chemical Reactivity; Mezey, P. G., Ed.; Kluwer Academic Publishers: Dordrecht, Netherlands, 2003; Vol. 24, pp 169−275.

(14) da Costa, L. M.; Stoyanov, S. R.; Gusarov, S.; Tan, T.; Gray, M. R.; Stryker, J. M.; Tykwinski, R.; Carneiro, J. W. M.; Seidl, P. R.; Kovalenko, A. Density functional theory investigation of the contributions of $\pi-\pi$ stacking and hydrogen-bonding interactions to the aggregation of model asphaltene compounds. *Energy Fuels* 2012, 26, 2727−2735.

(15) Seidl, P. R.; Oliveira, J. S. C.; Costa, L. M.; Stoyanov, S. R. A computational study on the steric effects of cyclic aliphatic moieties on the aggregation interactions in non-conventional petroleum constituents. *J. Phys. Org. Chem.* 2014, DOI: 10.1002/poc.3329.

(16) Stoyanov, S. R.; Yin, C.-X.; Gray, M. R.; Stryker, J. M.; Gusarov, S.; Kovalenko, A. Computational and experimental study of the structure, binding preferences, and spectroscopy of nickel(II) and

(17) Stoyanov, S. R.; Yin, C.-X.; Gray, M. R.; Stryker, J. M.; Gusarov, S.; Kovalenko, A. Density functional theory investigation of the effect of axial coordination and annelation on the absorption spectroscopy of nickel(II) and vanadyl porphyrins relevant to bitumen and crude oils. *Can. J. Chem.* 2013, 91, 872−878.

(18) Gillet, S.; Rubini, P.; Delpuech, J.; Escalier, J.; Valentim, P. Quantitative carbon-13 and proton nuclear magnetic resonance spectroscopy of crude oil and petroleum products. I. Some rules for obtaining a set of reliable structural parameters. *Fuel* 1981, 60, 221−226.

(19) Calemma, V.; Invanski, V.; Nali, P.; Scotti, M.; Montanari, R. Structural characterization of asphaltenes of different rings. *Energy Fuels* 1995, 9, 225−229.

(20) Andrew, A. B.; Edwards, J. C.; Pommerantz, A. E.; Mullins, O. C.; Nordlund, D.; Norinaga, K. Comparison of coal-derived and petroleum asphaltenes by ¹³C nuclear magnetic resonance, DEPT, and XRS. *Energy Fuels* 2011, 25, 3068−3076.

(21) Mullins, O. C. The modified Yen model. *Energy Fuels* 2010, 24, 2179−2207.

(22) Sheramata, J. M.; Gray, M. R.; Dettman, H. D.; McCaffrey, W. C. Quantitative molecular representation and sequential optimization of Athabasca asphaltenes. *Energy Fuels* 2004, 18, 1377−1384.

(23) Masuda, K.; Okuma, O.; Nishizawa, T.; Kanaji, M.; Matsumura, T. High-temperature n.m.r. analysis of aromatic units in asphaltenes and preasphaltenes derived from Victorian brown coal. *Fuel* 1996, 75, 295−299.

(24) Pinkston, D. S.; Duan, P.; Gallardo, V. A.; Habicht, S. C.; Tan, X. L.; Qian, K. N.; Gray, M.; Mullen, K.; Kenttamaa, H. I. Analysis of asphaltenes and asphaltene model compounds by laser-induced acoustic desorption/Fourier transform ion cyclotron ressonance mass spectrometry. *Energy Fuels* 2009, 23, 5564−5570.

(25) Brown, J. K.; Ladner, W. L. Hydrogen comparison in coal-like materials by resolution NMR spectroscopy. *Fuel* 1960, 39, 79−96.

(26) Seidl, P. R.; Yoneda, J. D.; Leal, K. Z. NMR investigation of steric effects in alkyl- and haloadamantanes. *J. Phys. Org. Chem.* 2005, 18, 162−166.

(27) Speight, J. A structural investigation of the constituents of Athabasca bitumen by proton magnetic resonance spectroscopy. *Fuel* 1970, 49, 76−77.

(28) Sato, S. Construction of asphaltene molecular model: A tool for average molecular structural analysis. *J. Jpn. Inst. Energy* 2007, 86, 792−799.

(29) Grimme, S. Accurate description of van der Waals complexes by density functional theory including empirical corrections. *J. Comput. Chem.* 2004, 25, 1463−1473.

(30) Mackie, I. D.; DiLabio, G. Interactions in large, polyaromatic hydrocarbon dimers: Application of density functional theory with dispersion corrections. *J. Phys. Chem. A* 2008, 112, 10968−10976.

(31) da Costa, L. M.; Stoyanov, S. R.; Gusarov, S.; Seidl, P. R.; Carneiro, J. W. M.; Kovalenko, A. Computational study of the effect of dispersion interactions on the thermochemistry of aggregation of fused polycyclic aromatic hydrocarbons as model asphaltene compounds in solution. *J. Phys. Chem. A* 2014, 118, 896−908.

(32) Ruiz-Morales, Y. HOMO−LUMO gap as index of molecular size and structure for polycyclic aromatic hydrocarbons (PAHs) and asphaltenes: A theoretical study. *J. Phys. Chem. A* 2002, 106, 11283−11308.

(33) Oliveira, J. S. C.; Quinteiro, L. C. N.; Albuquerque, M. G.; Seidl, P. R.; Leal, K. Z. Molecular dynamics simulation of asphaltenes models nanoaggregation. *Proceedings of the 12th International Conference on Petroleum Phase Behaviour and Fouling*; London, U.K., July 10−14, 2011.

(34) Chai, J.-D.; Head-Gordon, M. Long-range corrected hybrid density functionals with damped atom−atom dispersion corrections. *Phys. Chem. Chem. Phys.* 2008, 10, 6615−6620.

(35) (a) Rassolov, V. A.; Ratner, M. A.; Pople, J. A.; Redfern, P. C.; Curtiss, L. A. 6-31G* basis set for the third-row atoms. *J. Comput.*

Chem. **2001**, *22*, 976−984. (b) Frisch, M. J.; Pople, J. A.; Binkley, J. S. Self-consistent molecular orbital methods 25. Supplementary functions for Gaussian basis sets. *J. Chem. Phys.* **1984**, *80*, 3265−3269.

(36) Frisch, M. J.; Trucks, G. W.; Schlegel, H. B.; Scuseria, G. E.; Robb, M. A.; Cheeseman, J. R.; Scalmani, G.; Barone, V.; Mennucci, B.; Petersson, G. A.; Nakatsuji, H.; Caricato, M.; Li, X.; Hratchian, H. P.; Izmaylov, A. F.; Bloino, J.; Zheng, G.; Sonnenberg, J. L.; Hada, M.; Ehara, M.; Toyota, K.; Fukuda, R.; Hasegawa, J.; Ishida, M.; Nakajima, T.; Honda, Y.; Kitao, O.; Nakai, H.; Vreven, T.; Montgomery, J. A., Jr.; Peralta, J. E.; Ogliaro, F.; Bearpark, M.; Heyd, J. J.; Brothers, E.; Kudin, K. N.; Staroverov, V. N.; Kobayashi, R.; Normand, J.; Raghavachari, K.; Rendell, A.; Burant, J. C.; Iyengar, S. S.; Tomasi, J.; Cossi, M.; Rega, N.; Millam, M. J.; Klene, M.; Knox, J. E.; Cross, J. B.; Bakken, V.; Adamo, C.; Jaramillo, J.; Gomperts, R.; Stratmann, R. E.; Yazyev, O.; Austin, A. J.; Cammi, R.; Pomelli, C.; Ochterski, J. W.; Martin, R. L.; Morokuma, K.; Zakrzewski, V. G.; Voth, G. A.; Salvador, P.; Dannenberg, J. J.; Dapprich, S.; Daniels, A. D.; Farkas, Ö.; Foresman, J. B.; Ortiz, J. V.; Cioslowski, J.; Fox, D. J. *Gaussian 09, Revision D.01*; Gaussian, Inc.: Wallingford, CT, 2009.

(37) da Costa, L. M.; Hayaki, S.; Stoyanov, S. R.; Gusarov, S.; Tan, X.; Gray, M. R.; Stryker, J. M.; Tykwinski, R.; Carneiro, J. W. M.; Sato, H.; Seidl, P. R.; Kovalenko, A. 3D-RISM-KH molecular theory of solvation and density functional theory investigation of the role of water in the aggregation of model asphaltenes. *Phys. Chem. Chem. Phys.* **2012**, *14*, 3922−3934.

(38) Wolinski, K.; Hilton, J. F.; Pulay, P. Efficient implementation of the gauge-independent atomic orbital method for NMR chemical shift calculations. *J. Am. Chem. Soc.* **1990**, *112*, 8251−8260.

(39) Cheeseman, J. R.; Trucks, G. W.; Keith, T. A.; Frisch, M. J. A comparison of models for calculating nuclear magnetic resonance shielding tensors. *J. Chem. Phys.* **1996**, *104*, 5497−5509.

(40) Barone, V.; Cossi, M. Quantum calculation of molecular energies and energy gradients in solution by a conductor solvent model. *J. Phys. Chem. A* **1998**, *102*, 1995−2001.

(41) Cossi, M.; Rega, N.; Scalmani, G.; Barone, V. Energies, structures, and electronic properties of molecules in solution with the C-PCM solvation model. *J. Comput. Chem.* **2003**, *24*, 669−681.

(42) National Institute of Advanced Industrial Science and Technology (AIST). *Spectral Database for Organic Compounds (SDBS)*; ^{13}C *NMR; SDBS No.: 898; RN 71-43-2*; AIST: Tokyo, Japan, 2013; http://riodb01.ibase.aist.go.jp/sdbs/ (accessed Aug 15, 2014).

(43) National Institute of Advanced Industrial Science and Technology (AIST). *Spectral Database for Organic Compounds (SDBS)*; ^{13}C *NMR; SDBS No.: 518; RN 110-86-1*; AIST: Tokyo, Japan, 2013; http://riodb01.ibase.aist.go.jp/sdbs/ (accessed Aug 15, 2014).

(44) National Institute of Advanced Industrial Science and Technology (AIST). *Spectral Database for Organic Compounds (SDBS)*; ^{13}C *NMR; SDBS No.: 1430; RN 109-06-8*; AIST: Tokyo, Japan, 2013; http://riodb01.ibase.aist.go.jp/sdbs/ (accessed Aug 15, 2014).

(45) National Institute of Advanced Industrial Science and Technology (AIST). *Spectral Database for Organic Compounds (SDBS)*; ^{13}C *NMR; SDBS No.: 1567; RN 108-99-6*; AIST: Tokyo, Japan, 2013; http://riodb01.ibase.aist.go.jp/sdbs/ (accessed Aug 15, 2014).

(46) National Institute of Advanced Industrial Science and Technology (AIST). *Spectral Database for Organic Compounds (SDBS)*; ^{13}C *NMR; SDBS No.: 1824; RN 108-89-4*; AIST: Tokyo, Japan, 2013; http://riodb01.ibase.aist.go.jp/sdbs/ (accessed Aug 15, 2014).

(47) National Institute of Advanced Industrial Science and Technology (AIST). *Spectral Database for Organic Compounds (SDBS)*; ^{13}C *NMR; SDBS No.: 479; RN 110-02-1*; AIST: Tokyo, Japan, 2013; http://riodb01.ibase.aist.go.jp/sdbs/ (accessed Aug 15, 2014).

(48) National Institute of Advanced Industrial Science and Technology (AIST). *Spectral Database for Organic Compounds*

(SDBS); ^{13}C *NMR; SDBS No.: 3874; RN 1191-99-7*; AIST: Tokyo, Japan, 2013; http://riodb01.ibase.aist.go.jp/sdbs/ (accessed Aug 15, 2014).

(49) National Institute of Advanced Industrial Science and Technology (AIST). *Spectral Database for Organic Compounds (SDBS)*; ^{13}C *NMR; SDBS No.: 1313; RN 110-00-9*; AIST: Tokyo, Japan, 2013; http://riodb01.ibase.aist.go.jp/sdbs/ (accessed Aug 15, 2014).

(50) National Institute of Advanced Industrial Science and Technology (AIST). *Spectral Database for Organic Compounds (SDBS)*; ^{13}C *NMR; SDBS No.: 1350; RN 91-20-3*; AIST: Tokyo, Japan, 2013; http://riodb01.ibase.aist.go.jp/sdbs/ (accessed Aug 15, 2014).

(51) National Institute of Advanced Industrial Science and Technology (AIST). *Spectral Database for Organic Compounds (SDBS)*; ^{13}C *NMR; SDBS No.: 907; RN 119-64-2*; AIST: Tokyo, Japan, 2013; http://riodb01.ibase.aist.go.jp/sdbs/ (accessed Aug 15, 2014).

(52) National Institute of Advanced Industrial Science and Technology (AIST). *Spectral Database for Organic Compounds (SDBS)*; ^{13}C *NMR; SDBS No.: 1195; RN 120-12-7*; AIST: Tokyo, Japan, 2013; http://riodb01.ibase.aist.go.jp/sdbs/ (accessed Aug 15, 2014).

(53) National Institute of Advanced Industrial Science and Technology (AIST). *Spectral Database for Organic Compounds (SDBS)*; ^{13}C *NMR; SDBS No.: 870; RN 85-01-8*; AIST: Tokyo, Japan, 2013; http://riodb01.ibase.aist.go.jp/sdbs/ (accessed Aug 15, 2014).

(54) National Institute of Advanced Industrial Science and Technology (AIST). *Spectral Database for Organic Compounds (SDBS)*; ^{13}C *NMR; SDBS No.: 878; RN 129-00-0*; AIST: Tokyo, Japan, 2013; http://riodb01.ibase.aist.go.jp/sdbs/ (accessed Aug 15, 2014).

(55) National Institute of Advanced Industrial Science and Technology (AIST). *Spectral Database for Organic Compounds (SDBS)*; ^{13}C *NMR; SDBS No.: 1373; RN 191-07-1*; AIST: Tokyo, Japan, 2013; http://riodb01.ibase.aist.go.jp/sdbs/ (accessed Aug 15, 2014).

(56) Huheey, J. E.; Keiter, E. A.; Keiter, R. L. *Inorganic Chemistry: Principles of Structure and Reactivity*; HarperCollins: New York, 1993.

(57) Merino, G.; Heine, T.; Seifert, G. The induced magnetic field in cyclic molecules. *Chem.—Eur. J.* **2004**, *10*, 4367−4371.

(58) Gomes, J. A. N. F.; Mallion, R. B. Aromaticity and ring currents. *Chem. Rev.* **2001**, *101*, 1349−1384.

(59) Badu, S.; Pimienta, I. S. O.; Orendt, A. M.; Pugmire, R. J.; Facelli, J. C. Modeling of asphaltenes: Assessment of sensitivity of ^{13}C solid state NMR to molecular structure. *Energy Fuels* **2012**, *26*, 2161−2167.